Journal of Biomedical Optics

SPIEDigitalLibrary.org/jbo

Optimization of the open-loop liquid crystal adaptive optics retinal imaging system

Ningning Kong
Chao Li
Mingliang Xia
Dayu Li
Yue Qi
Li Xuan

SPIE

Optimization of the open-loop liquid crystal adaptive optics retinal imaging system

Ningning Kong,[a,b,c] Chao Li,[d] Mingliang Xia,[b] Dayu Li,[b] Yue Qi,[a,b,c] and Li Xuan[a]
[a]State Key Laboratory of Applied Optics, Changchun Institute of Optics, Fine Mechanics and Physics, Changchun, Jilin 130033, China
[b]Suzhou Institute of Biomedical Engineering and Technology, Chinese Academy of Sciences, Suzhou, Jiangsu 215163, China
[c]Graduate University of the Chinese Academy of Sciences, Beijing 100039, China
[d]Institute of Medical Equipment, Academy of Military Medical Sciences, Tianjin 300161, China

Abstract. An open-loop adaptive optics (AO) system for retinal imaging was constructed using a liquid crystal spatial light modulator (LC-SLM) as the wavefront compensator. Due to the dispersion of the LC-SLM, there was only one illumination source for both aberration detection and retinal imaging in this system. To increase the field of view (FOV) for retinal imaging, a modified mechanical shutter was integrated into the illumination channel to control the size of the illumination spot on the fundus. The AO loop was operated in a pulsing mode, and the fundus was illuminated twice by two laser impulses in a single AO correction loop. As a result, the FOV for retinal imaging was increased to 1.7-deg without compromising the aberration detection accuracy. The correction precision of the open-loop AO system was evaluated in a closed-loop configuration; the residual error is approximately 0.0909λ (root-mean-square, RMS), and the Strehl ratio ranges to 0.7217. Two subjects with differing rates of myopia (-3D and -5D) were tested. High-resolution images of capillaries and photoreceptors were obtained. [DOI: 10.1117/1.JBO.17.2.026001]

Keywords: adaptive optics; retinal imaging; open-loop; field of view; liquid crystal spatial light modulator.

Paper 11171 received Apr. 8, 2011; revised manuscript received Dec. 5, 2011; accepted for publication Dec. 5, 2011; published online Mar. 22, 2012.

1 Introduction

The retina of the human eye is an important organ that can be noninvasively observed *in vivo*. Retina microscopic imaging is important in vision science and aids in the early clinic diagnoses of retinal diseases.[1–3] However, the resolution of retinal images is limited by ocular aberrations. To overcome this obstacle, Liang et al. developed an adaptive optics (AO) retinal imaging system to compensate for dynamic ocular aberrations and nearly achieved diffraction-limited resolution.[4,5] Afterward, there was a remarkable expansion in the research and application of ophthalmoscopes equipped with AO systems for human retinal imaging.[6,7] This technology provided an opportunity to noninvasively image the retina at a microscopic cellular level.

The key components of the AO system are the wavefront sensor and compensator. The Shack-Hartmann wavefront sensor (SH-WFS) is the most popular wavefront measurement device used in AO systems. A deformable mirror (DM) is the first choice for the compensator in an AO system and has wide application in both astronomy and retinal imaging.[8,9] However, this mirror's application in ophthalmology is restricted by its high price and bulky physical structure. Apart from DM, low cost and compact compensators, such as liquid crystal spatial light modulator (LC-SLM)[10,11] and micro-electro-mechanical system (MEMS),[12] are also available.

In this study, we developed a retinal imaging AO system using LC-SLM as the wavefront compensator. LC-SLM modulates the phase of the light beam by tuning the apparent refractive index with an applied voltage. As wavefront compensator, LC-SLM has a number of attractive advantages, such as high spatial resolution, compactness, low drive voltage, and low cost. The LC-SLM also has a wider correction depth to compensate for the large ocular aberrations of the phase unwrapping method.[13] The first results of LC-SLM-based AO system for a -5D myopia subject have been reported by Mu et al.[14]

However, LC-SLM also has many wavefront compensation limitations, such as a long response time.[15] In this experiment, we chose the nematic LC-SLM manufactured by Boulder Nonlinear Systems, Inc. (BNS, CO, USA). The spatial resolution of this LC-SLM is 512×512 pixels, and the response time is less than 13 ms, which is adequate for the intended application. Due to the dispersion of the liquid crystal, the phase modulation performance of the LC-SLM also depends on the wavelength of the incident light,[16] which results in a narrow working spectrum bandwidth. Therefore, only one laser source was employed in this experiment.

The LC-SLM can only modulate polarized light, which means that more than half of the light backscattered from the fundus will be lost. Unfortunately, the backscattered light is weak. Therefore, ensuring that enough light is reflected from the eye and is detected by the imaging Charge Coupled Device (CCD) required increasing the energy entering the eye. However, if the energy source entering the human eye is too great, it can be harmful. Many methods for solving this problem have been proposed,[17,18] and an open-loop AO system was adopted in this experiment. The energy efficiency of the open-loop AO system is increased to more than twice that of the closed-loop LC-SLM-based AO system.

Address all correspondence to: Li Xuan, State Key Laboratory of Applied Optics, Changchun Institute of Optics, Fine Mechanics and Physics, Chinese Academy of Sciences, Changchun, Jilin 130033, China. Tel: +086 431 86176316; Fax: +086 431 85682346; E-mail: xuanli_ao@163.com

0091-3286/2012/$25.00 © 2012 SPIE

In our previous experiment, the imaging FOV was only about 0.75-deg[19] because it was limited by the SH-WFS. To enlarge the imaging FOV, a modified shutter was incorporated into the illumination channel in conjugation with the fundus, and the FOV was increased to 1.7-deg. Furthermore, the single light source was operated in a pulsing mode to avoid illuminating the eye during the data processing period. Details of the proposed AO system are discussed in later sections.

2 Experimental Setup and Methods

A schematic diagram of the open-loop AO system is shown in Fig. 1. The imaging system used the subjective accommodation of the human eye to correct the defocus aberration, as we have previously described.[14,19]

A customized SH-WFS was employed in the AO system to measure the ocular aberration. The focal length and diameter of the sub-aperture are 6 mm and 300 μm, respectively, and the aperture of the SH-WFS is 4.2 mm. The measurement of accuracy can reach $1/100\lambda$ (root-mean-square, RMS) in relative mode.

The LC-SLM (XY series Spatial Light Modulator, Boulder Nonlinear Systems, CO, USA) was used as the wavefront compensator in the system and has a resolution of 512×512 pixels over its 7.68×7.68 mm aperture, with a response time that can reach 13 ms at 35 °C.

The configuration of the proposed open-loop AO system was similar to the closed-loop AO system using a DM or MEMS as a compensator. However, it should be noted that in the LC-SLM-based closed-loop AO system, there was a polarizer placed in front of the eye to select the linearly polarized light that was matched with the LC-SLM[20,21] because the LC-SLM can only modulate linearly polarized light. In the open-loop AO system, as shown in Fig. 1, a polarized beam splitter (PBS) was positioned behind the LC-SLM. The light reflected from the eye and projected onto the LC-SLM was divided into two beams with orthogonal polarization direction. The *S* polarization component, which was reflected by the PBS, was parallel with the modulation direction of the LC-SLM; therefore, it can be modulated and ultimately strike the imaging CCD. The *P* polarization component, which was perpendicular to the modulation direction of the LC-SLM, cannot be modulated and thus went into the SH-WFS for wavefront sensing. As a result, the residual aberration after correction cannot be detected during the open-loop correction. That is, in the open-loop correction, the SH-WFS measures the total ocular aberrations and the LC-SLM corrects them in real time. The LC-SLM has excellent repeatability, linearity and high precision for generating a desired wavefront,[22,23] which makes open-loop control possible. The eye pupil was conjugated with the lenslet array planes of both the SH-WFS and the LC-SLM by lenses L1, L2, and L3. A hole was placed at the position of the fundus image to block the high-order diffraction light introduced by the LC-SLM and the stray environmental light.

Images of the photoreceptor have high contrast over a wide range of wavelengths.[24] In this study, an 808 nm laser (Infrared Diode Laser, CNI, Changchun, China) was chosen for photoreceptor imaging because it causes less damage to retinal tissue and reflects more from the retina than do shorter wavelengths.[25] Moreover, this laser appears less bright, which is more comfortable for the subject. A 561 nm laser (LD Pumped All-Solid-State Laser, CNI, Changchun, China) was used as the illumination source for capillary imaging because the absorption of the blood at this spectrum is high, and the capillaries become more visible against the bright background. Accordingly, different LC-SLMs corresponding to different light sources were chosen as compensators because of the narrow working bandwidth of the LC-SLM. The speckle noise that originates from the coherence of the laser source masks retinal information in the recorded image; therefore, a rotating diffuser (thin frosted glass) was placed in front of the laser to reduce the speckle noise.[26]

In conventional AO systems with two light sources, there is a longitudinal focal shift between the imaging and the wavefront sensing beams that is caused by the intrinsic chromatic aberrations of the eye. In general, this focal shift is compensated

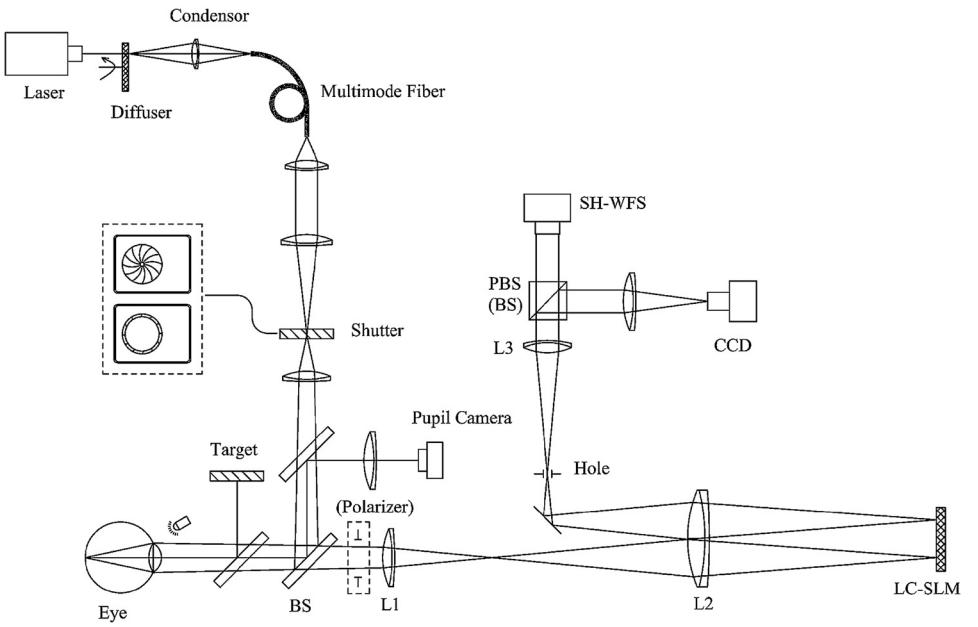

Fig. 1 A schematic of the open-loop AO retinal imaging system; in the open-loop configuration, there is no polarizer between BS and L1, and the light splitter before the imaging CCD and the SH-WFS is a polarized beam splitter (PBS). If we insert a polarizer between BS and L1, as shown in the dotted-line box and replace the PBS with the beam splitter (BS), the open-loop configuration will switch to the closed-loop configuration. The diagram of the shutter is in the dotted-line box on the left of the shutter: the upper diagram denotes the shutter closed, the lower one denotes the shutter opened.

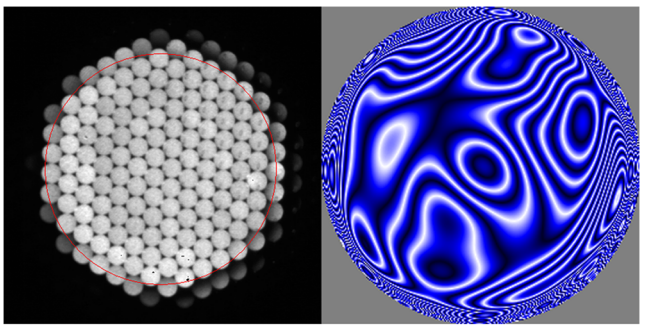

Fig. 2 (a) The spots array of the SH-WFS and (b) the corresponding wavefront map. The FOV of the illumination area on the fundus is 1.7-deg. The red circle in (a) denotes the mask of the SH-WFS.

for by translating the imaging CCD axially.[27] In this system, there was only one light source; therefore, the longitudinal focal shift between the imaging and the wavefront sensing beams was eliminated.

In the AO retinal imaging system, the aberration measurement and retinal imaging have different requirements for the size of the illumination area on the fundus. For retinal imaging, a large field size is always advantageous, but it should be noted that the imaging FOV is restricted by the isoplanatic angle of the human eye. If the imaging FOV is greater than the isoplanatic angle, then the adaptive compensation effect will be lost.[28–30] However, the illumination spot projected on the retina should be a "point source" to ensure the wavefront sensing accuracy. If the illumination area on the fundus is too large, the light spots on the SH-WFS will link to each other and result in detection error, as shown in Fig. 2. To solve this problem, two light sources (one for wavefront sensing and one for retinal imaging) can be used. There was only one light source in our system, however, and the size of the illumination area on the fundus for the wavefront sensing is the same as that for the retinal imaging. To ensure the detection accuracy of the SH-WFS, the illumination spot on the fundus in our previous experiment was approximately 0.75-deg for both the retinal imaging and wavefront sensing.[19] To enlarge the FOV of the retinal imaging without decreasing the wavefront sensing accuracy of the SH-WFS, a modified mechanical shutter was used to control the FOV. The shutter was conjugated to the fundus with a hole in the shutter center, as shown in the dotted-line box on the left of the shutter in Fig. 1. The size of the illumination area on the fundus can be adjusted by changing the clear aperture of the shutter. When ocular aberrations were detected, the shutter was closed. The size of the illumination area on the fundus was restricted by the small hole in the shutter. The smaller hole of the shutter for wavefront sensing can be easily determined. First, the size of the laser spot projected on the fundus should be smaller than the isoplanatic patch of human eye, and meanwhile, the light spot on the SH-WFS could not link to each other. In the experiment, the diameter of the small hole was 0.9 mm and results in an approximately 0.4-deg illumination spot on the fundus. The shutter was open for the retinal imaging, and the illumination spot size was increased to 1.7-deg, which was approximately equal to the isoplanatic angle of the human eye.

In our previous experiment, the eye suffered laser irradiance during the data processing period, and the backscattered light from the eye was useless for both aberration detection and retina imaging. To avoid unnecessary illumination during the data processing period, the laser was activated in pulses a customized electric circuit. The timing sequence of the system is shown in Fig. 3. At the beginning of the AO loop, the SH-WFS was activated first, which caused the laser pulse to illuminate the retina. The duration of the laser pulse was 13 ms. The backscattered light from the retina traveled back through the pupil, entered the AO system, and was ultimately sampled by the SH-WFS. The aberration was detected by the SH-WFS, and the slope signal was sent to the host computer. The wavefront was reconstructed based on Zernike modes. The compensation signal was calculated by the command matrix and sent to the LC-SLM. This process lasted a total of 13 ms. Meanwhile, the shutter was triggered to open, which allowed the entire beam to pass through the shutter and enlarged the field angle to 1.7-deg. The response time of the LC-SLM was 13 ms, and the ocular aberration was compensated for by the LC-SLM. The imaging CCD was subsequently triggered to expose and the eye was again illuminated by the laser. The duration of the laser pulse was 7 ms, and the exposure time of the CCD was set to 8 ms, which was short enough to arrest the motion of the retina.[27] The entire loop was completed in 49 ms. The corresponding frequency was approximately 20 Hz, which was sufficient to correct the dynamic ocular aberration.[31] It is well-known that the eye is sensitive to light at a wavelength of 561 nm and that the pupil will shrink when the eye is illuminated by the laser pulse. In this experiment, the interval of the laser pulses between the wavefront sensing and retina imaging

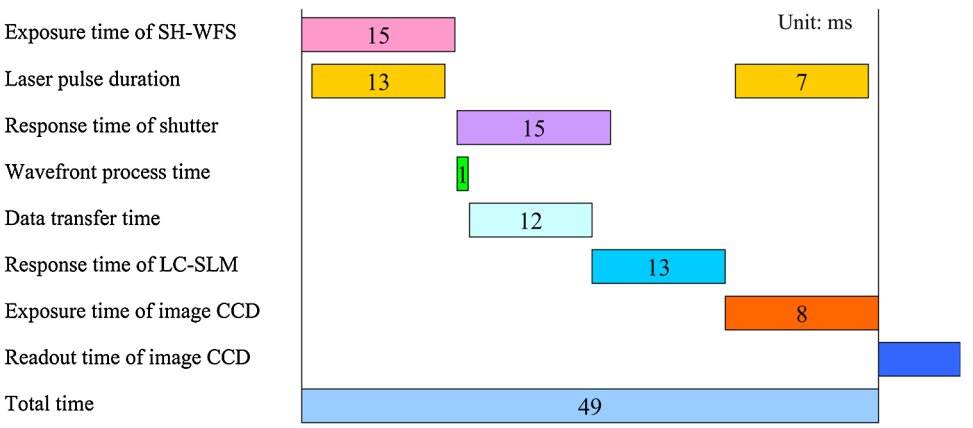

Fig. 3 The sequential chart of the open-loop AO system.

was 13 ms. This period was short enough that the eye could not react; therefore, there was no impact on retinal imaging.

The exposure levels at the cornea for the 561 and the 808 nm lasers were 0.3 and 0.5 mw, respectively. Both of these exposures were less than 1/10 of the maximum permissible exposure (MPE) recommended by ANSI.[32] The fixation target was a commercial 5-inch LCD, and the target icon was a green cross on a black background that was placed 200 mm away from the eye. Under the experimental illumination conditions, the subjects' pupils were dilated larger than the 6 mm design stop size without using drug dilation or cycloplegia.

3 Results

The open-loop correction precision for dynamic ocular aberration was tested first. In the open-loop AO system, SH-WFS was blinded to the residual wavefront error after the AO correction; therefore, we used the open-loop control method on the closed-loop optical system to evaluate its correction precision. The configuration of the closed-loop AO system is shown in Fig. 1; it was similar to the system proposed by Mu et al.[14] Meanwhile, the closed-loop AO correction was also performed, so that we could directly compare the open-loop correction effect with the closed-loop correction. The wavelength of the illumination source was 808 nm, and photoreceptor images before and after the AO correction was obtained. One male (LC, aged 27 years, -5D myopia) was recruited for the experiment. The original wavefront map of the ocular aberration is shown in Figs. 4(a)–4(c) shows the residual wavefront errors after the open-loop correction and closed-loop correction, respectively, for CL. The residual wavefront errors after the open-loop and closed-loop corrections were 0.0909λ (RMS) and 0.0673λ (RMS), respectively, and the corresponding Strehl ratios were 0.7217 and 0.8363, respectively. The retinal images before and after correction are shown in Fig. 5. To measure the residual error after the AO correction, the imaging FOV was approximately 0.65-deg. The single photoreceptor could be resolved after the AO correction, and the image quality after the open-loop correction was as good as that observed after the closed-loop correction. Thus, we concluded that the resolution of the optical system after the open-loop AO correction nearly achieves the diffraction limit resolution; although the Strehl ratio after the open-loop AO correction is lower than that after the closed-loop correction.

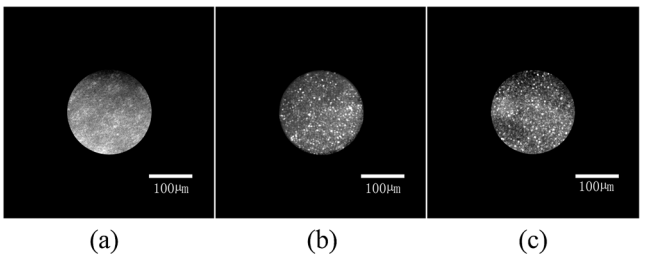

Fig. 5 Photoreceptor images before and after the AO correction; (a) before the AO correction; (b) after the open-loop AO correction; (c) after the closed-loop AO correction. The 0.65-deg FOV was illuminated by the 808 nm laser; the mosaic of bright dots in (b) and (c) are the photoreceptors; the scale bars represent 100 μm.

The capillary and photoreceptor imaging experiments were performed using the open-loop AO system. The two subjects tested were DY (-3D, age 31) and LC (-5D, age 27). The image area on the retina was about 1.5-deg from the fovea. Figure 6 shows the ocular aberrations of the two subjects, which were measured using wavelengths of 561 nm and 808 nm, respectively. The major chromatic aberration is defocus, which is consistent with the conclusion of Marcos and Burns.[33]

For capillary imaging, the eye was illuminated by the 561 nm laser. The images of retina capillaries of the two subjects before and after the AO compensation are shown in Fig. 7. The image quality was significantly improved after the AO compensation, and the tube structure of the capillaries can be clearly resolved.

The wavelength of the illumination source for photoreceptor imaging was 808 nm. The photoreceptor images from both subjects across 1.7-deg FOV, with and without AO compensation, are shown in Fig. 8. In Figs. 8(a) and 8(b), we could not visualize any significant contrast or the microscopic structure of retina without the AO compensation, although most of the defocus was compensated for by subjective accommodation. After AO compensation, the photoreceptors could be resolved clearly, as is shown in Figs. 8(c) and 8(d). To quantify the improvement of the image quality with the open-loop AO compensation, Fig. 9 shows the computed average power spectra for LC, with and without AO compensation. As shown in the figure, the power spectrum of the image is significantly improved after the AO compensation, especially for the cone photoreceptors for which the spatial frequency ranged from 70 to 90 cycles/deg.

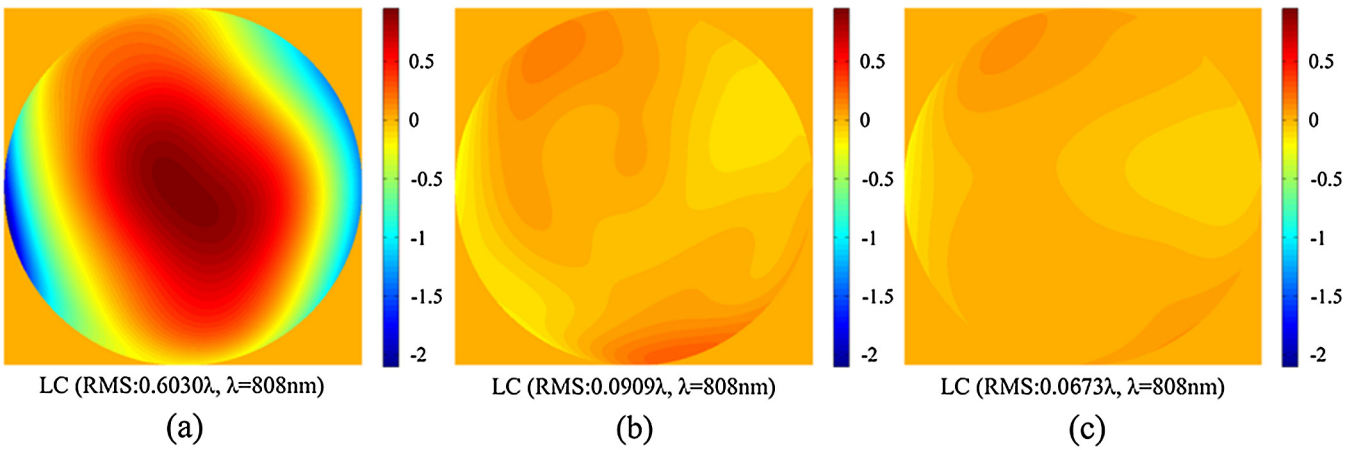

Fig. 4 The ocular aberrations for LC, before and after the AO correction; (a) before the AO correction; (b) after the open-loop AO correction; (c) after the closed-loop AO correction.

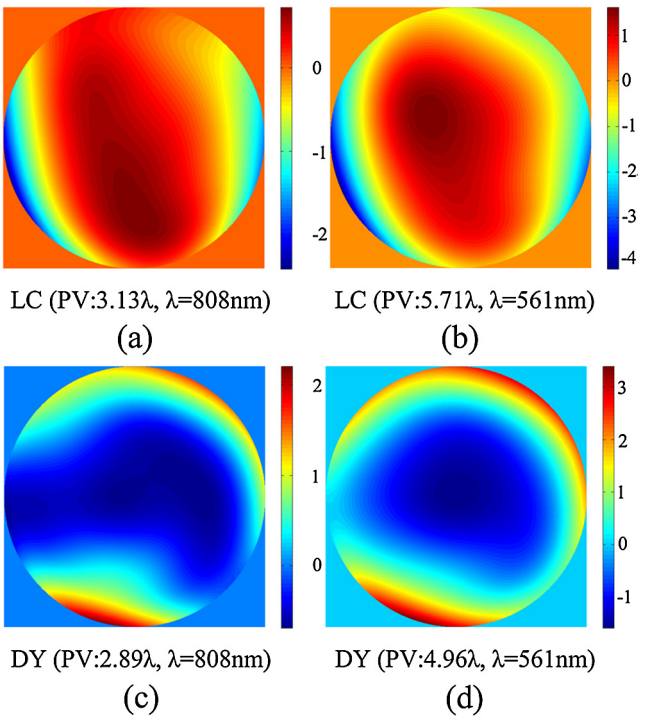

Fig. 6 The ocular aberration of LC (a, b) and DY (c, d), as measured by 561 and 808 nm lasers, respectively.

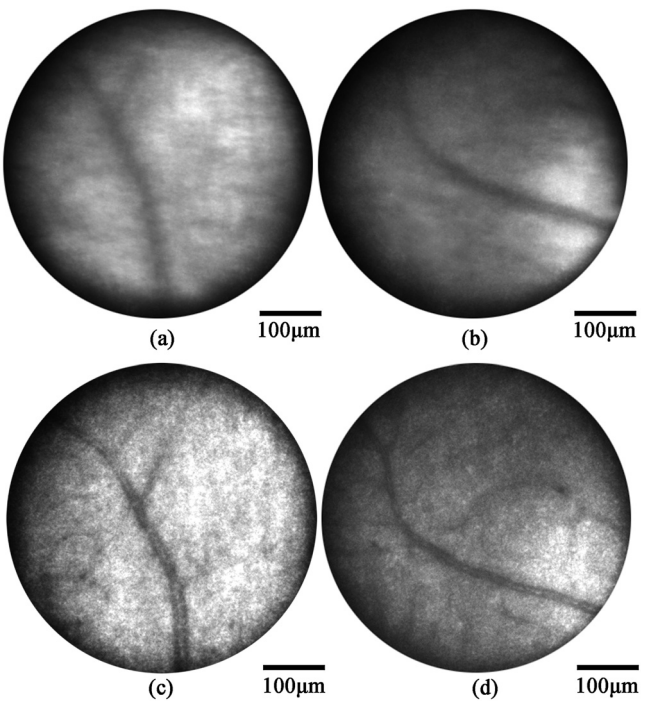

Fig. 7 Retinal capillary images before the AO compensation (a, b) and after the AO compensation (c, d) for the subjects LC and DY, respectively. The 1.7-deg FOV was illuminated by the 561 nm laser. The scale bars represent 100 μm.

Finally, continuous correction and imaging for the photoreceptors were performed. The results are shown in Video 1. The video was recorded at 20 frames per second (fps) for approximately 4.5 s but is displayed slowly at 15 fps to ensure that every frame is clear. As can be seen in Video 1, although most of the

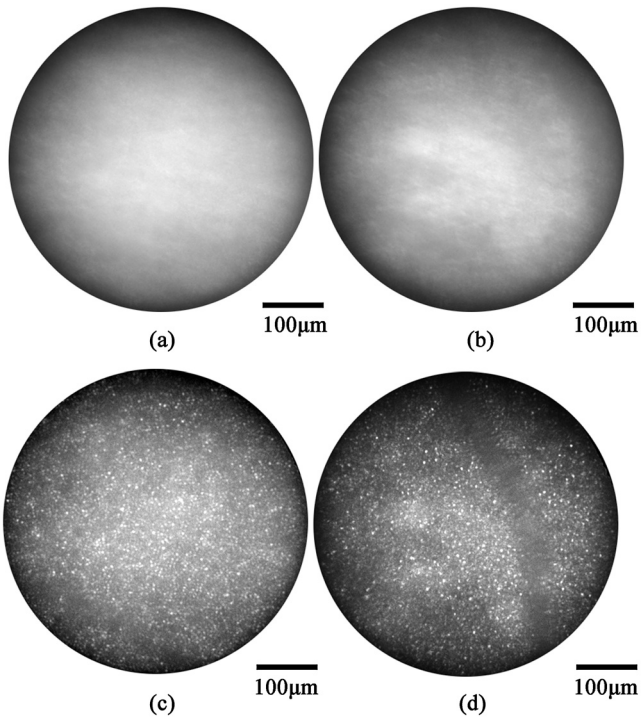

Fig. 8 Photoreceptor images before the AO compensation (a, b) and after the AO compensation (c, d) for the subjects LC and DY, respectively. The 1.7-deg FOV was illuminated by the 808 nm laser. The dark, hazy sub-regions in the image (d) are probably the shadows of small retinal vessels projected onto the photoreceptor layer. The scale bars represent 100 μm.

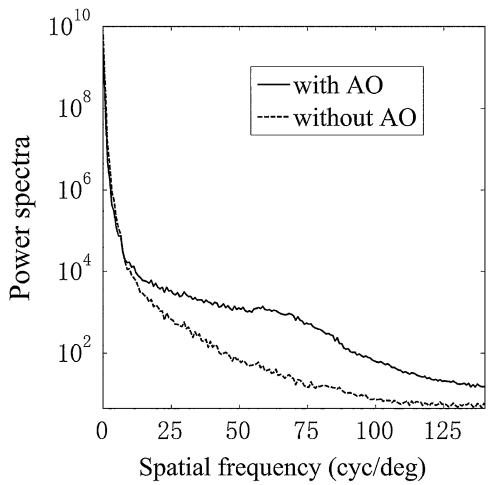

Fig. 9 The radially averaged cone power spectra for LC with and without AO compensation.

defocus was corrected by the eye's subjective accommodation when the AO was deactivated, the fundus image does not show any significant contrast or microscopic structure. With AO compensation, both the higher and lower (residual defocus and astigmatism) order aberrations were corrected, and the photoreceptors within the 1.7-deg FOV can be clearly resolved. The illumination source for the capillary imaging was 561 nm, which is a wavelength at which the human eye is sensitive; thus, we could not record the video for capillary imaging.

The resolution of the fundus imaging system was significantly improved by the open-loop correction. The quality of

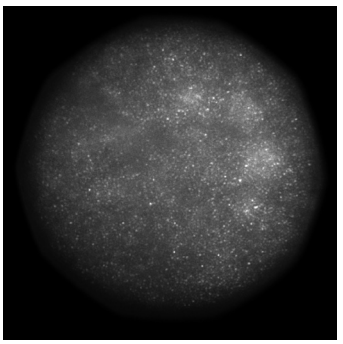

Video 1 Raw videos of the photoreceptors of LC, measured before and after the AO correction (QuickTime 23.5 MB]) [URL: http://dx.doi.org/10.1117/1.JBO.17.2.026001.1].

the retina image, including resolution, brightness and contrast, was as good as that obtained from the closed-loop AO system.[14,27] However, the contrast of the retina images was poorer than that of the images obtained through a AO-SLO system[34] because the AO system cannot filter out unwanted light reflected by the other layers of the retina.

4 Conclusion

In previous open-loop LC-SLM-based AO retinal imaging systems, the imaging FOV was restricted by the SH-WFS. We investigate a novel optimized open-loop AO retinal imaging system that uses a modified mechanical shutter to achieve a significantly larger imaging FOV. Retinal images were successfully collected with the exposure duration set to 20 ms for a 1.7-deg retinal patch. The correction precision of the open-loop AO system for dynamic ocular aberrations was tested. The residual error after the open-loop correction was 0.0909λ (RMS), and the Strehl ratio can reach 0.7217. With the open-loop correction, the resolution of the optical system was nearly diffraction-limited. With the subjective accommodation method, a single photoreceptor and the tube structure of the capillaries could be clearly resolved in two experimental subjects.

Acknowledgments

This work has been supported by National Natural Science Foundation of China (Grant Nos. 60736042, 1174274, and 1174279), Natural Science Foundation of Jiangsu Province, China (Grant No. SBK201020903), and Plan for Scientific and Technology Development of Suzhou, China (Grant No. ZXS201001).

References

1. R. S. Jonnal et al., "Imaging outer segment renewal in living human cone photoreceptors," *Opt. Express* **18**(5), 5257–5270 (2010).
2. Y. Kitaguchi et al., "Adaptive optics fundus camera to examine localized changes in the photoreceptor layer of the fovea," *Ophthalmology* **115**(10), 1771–1777 (2008).
3. Z. Zhong et al., "In vivo measurement of erythrocyte velocity and retinal blood flow using adaptive optics scanning laser ophthalmoscopy," *Opt. Express* **16**(17), 12746–12756 (2008).
4. J. Liang et al., "Objective measurement of wave aberrations of the human eye with the use of a Hartmann-Shack wave-front sensor," *J. Opt Soc. Am. A* **11**(7), 1949–1957 (1994).
5. J. Liang, D. R. Williams, and D. T. Miller, "Supernormal vision and high-resolution retinal imaging through adaptive optics," *J. Opt. Soc. Am. A* **14**(11), 2884–2892 (1997).
6. U. Wittrock et al., "A high-resolution adaptive optics fundus imager," in *Adaptive Optics for Industry and Medicine*, pp. 333–341, Springer, Berlin Heidelberg (2005).
7. M. Bass, J. M. Enoch, and V. Lakshminarayanan, *Handbook of Optics, Volume III—Vision and Vision Optics*, 3rd ed., McGraw-Hill, New York, pp. 15.11–15.30 (2010).
8. H. Hofer et al., "Improvement in retinal image quality with dynamic correction of the eye's aberrations," *Opt. Express* **8**(11), 631–643 (2001).
9. G. Rodrigues et al., "Modular bimorph mirrors for adaptive optics," *Opt. Eng.* **48**(3), 034001 (2009).
10. L. N. Thibos and A. Bradley, "Use of liquid-crystal adaptive-optics to alter the refractive state of the eye," *Optom. Vis. Sci.* **74**(7), 581–587 (1997).
11. P. Prieto et al., "Adaptive optics with a programmable phase modulator: applications in the human eye," *Opt. Express* **12**(17), 4059–4071 (2004).
12. Y. Zhang, S. Poonja, and A. Roorda, "MEMS-based adaptive optics scanning laser ophthalmoscopy," *Opt. Lett.* **31**(9), 1268–1270 (2006).
13. Y. Liu et al., "Correction for large aberration with phase-only liquid-crystal wavefront corrector," *Opt. Eng.* **45**(12), 128001 (2006).
14. Q. Q. Mu et al., "Accommodation-based liquid crystal adaptive optics system for large ocular aberration correction," *Opt. Lett.* **33**(24), 2898–2900 (2008).
15. P. Artal, F. Vargas-Martin, and P. M. Prieto, "Correction of the aberrations in the human eye with a liquid-crystal spatial light modulator: limits to performance," *J. Opt. Soc. Am. A* **15**(9), 2552–2562 (1998).
16. S. T. Wu, "Birefringence dispersions of liquid crystals," *Phys. Rev. A* **33**(2), 1270–1274 (1986).
17. H. W. Ren, Y. H. Lin, and S. T. Wu, "Polarization-independent and fast-response phase modulators using double-layered liquid crystal gels," *Appl. Phys. Lett.* **88**(6), 0611231–0611233 (2006).
18. G. D. Love, "Liquid-crystal phase modulator for unpolarized light," *Appl. Opt.* **32**(13), 2222–2223 (1993).
19. C. Li et al., "High-resolution retinal imaging through open-loop adaptive optics," *J. Biomed. Opt.* **15**(4), 0460091–0460096 (2010).
20. J. Bao-Guang et al., "Simulated human eye retina adaptive optics imaging system based on a liquid crystal on silicon device," *Chin. Phys. B* **17**(12), 4529–4532 (2008).
21. Q. Mu et al., "Liquid Crystal based adaptive optics system to compensate both low and high order aberrations in a model eye," *Opt. Express* **15**(4), 1946–1953 (2007).
22. G. D. Love, "Wave-front correction and production of Zernike modes with a liquid-crystal spatial light modulator," *Appl. Opt.* **36**(7), 1517–1524 (1997).
23. J. D. Schmidt, M. E. Goda, and B. D. Duncan, "Aberration production using a high-resolution liquid-crystal spatial light modulator," *Appl. Opt.* **46**(13), 2423–2433 (2007).
24. S. S. Choi et al., "Effect of wavelength on in vivo images of the human cone mosaic," *J. Opt. Soc. Am. A* **22**(12), 2598–2605 (2005).
25. F. C. Delori and K. P. Pflibsen, "Spectral reflectance of the human ocular fundus," *Appl. Opt.* **28**(6), 1061–1077 (1989).
26. C. Li et al., "Laser speckle reduction in retina imaging illumination," *Acta Opt. Sin.* **28**(12), 2245–2249 (2008).
27. J. Rha et al., "Adaptive optics flood-illumination camera for high speed retinal imaging," *Opt. Express* **14**(10), 4552–4569 (2006).
28. T. O. Salmon and C. van de Pol, "Normal-eye Zernike coefficients and root-mean-square wavefront errors," *J. Cataract Refract. Surg.* **32**(12), 2064–2074 (2006).
29. A. Dubinin et al., "Human eye anisoplanatism: eye as a lamellar structure," *Proc. SPIE*, **6138**, 613813 (2006)
30. A. Dubinin et al., "Anisoplanatism in human retina imaging," *Proc. SPIE*, **5894**, 589409 (2005).
31. H. Hofer et al., "Dynamics of the eye's wave aberration," *J. Opt. Soc. Am. A* **18**(3), 497–506 (2001).
32. American National Standards Institute, "*American National Standard for the Safe Use of Lasers*," ANSI Z136.1-2007, Laser Institute of America, Orlando, FL (2007).
33. S. Marcos et al., "A new approach to the study of ocular chromatic aberrations," *Vis. Res.* **39**(26), 4309–4323 (1999).
34. A. Roorda et al., "Adaptive optics scanning laser ophthalmoscopy," *Opt. Express* **10**(9), 405–412 (2002).